Social contagions with communication channel alternation on multiplex networks

Wei Wang,[1,2] Ming Tang,[3,4,*] H. Eugene Stanley,[5] and Lidia A. Braunstein[6,5]

[1]*Cybersecurity Research Institute, Sichuan University, Chengdu 610065, China*
[2]*Big Data Research Center, University of Electronic Science and Technology of China, Chengdu 610054, China*
[3]*School of Information Science and Technology, East China Normal University, Shanghai, 200241, China*
[4]*Shanghai Key Laboratory of Multidimensional Information Processing, East China Normal University, Shanghai 200241, China*
[5]*Center for Polymer Studies and Department of Physics, Boston University, Boston, Massachusetts 02215, USA*
[6]*Instituto de Investigaciones Físicas de Mar del Plata (IFIMAR)-Departamento de Física, Facultad de Ciencias Exactas y Naturales, Universidad Nacional de Mar del Plata-CONICET, Funes 3350, (7600) Mar del Plata, Argentina*

Internet communication channels, e.g., Facebook, Twitter, and email, are multiplex networks that facilitate interaction and information-sharing among individuals. During brief time periods users often use a single communication channel, but then communication channel alteration (CCA) occurs. This means that we must refine our understanding of the dynamics of social contagions. We propose a non-Markovian behavior spreading model in multiplex networks that takes into account the CCA mechanism, and we develop a generalized edge-based compartmental method to describe the spreading dynamics. Through extensive numerical simulations and theoretical analyses we find that the time delays induced by CCA slow the behavior spreading but do not affect the final adoption size. We also find that the CCA suppresses behavior spreading. On two coupled random regular networks, the adoption size exhibits hybrid growth, i.e., it grows first continuously and then discontinuously with the information transmission probability. CCA in Erdős-Rényi–Scale-Free (ER-SF) multiplex networks in which two subnetworks are ER and SF introduces a crossover from continuous to hybrid growth in adoption size versus information transmission probability. Our results extend our understanding of the role of CCA in spreading dynamics and may elicit further research.

I. INTRODUCTION

Numerous social communication platforms, including Facebook, Twitter, and email, are a part of the current worldwide information explosion. These platforms taken together behave as a network of networks (NON) in which each communication platform functions as a subnetwork [1–4]. These NONs can be multilayer, interdependent, or multiplex. In interdependent networks the functionality of the components in one network depends on the functionality of nodes in other networks. A multiplex network is a special NON case in which each agent can be present in more than one layer. Extensive studies of cascading failure, evolutionary games, synchronization, and spreading dynamics have found that the dynamics of NONs differ greatly from those of single networks [5–11]. For example, Buldyrev *et al.* found a first-order percolation phase transition in interdependent networks that is qualitatively different from the second-order phase transition in single networks [7]. Baxter *et al.* found a hybrid phase transition in the percolation phase transition on multiplex networks [12].

Spreading dynamics in complex networks can be classified as either biological or social contagions. In biological contagions, such as epidemic spreading, researchers have found that multilayer networks promote spreading [8,9], induce the

coexistence of mixed phase transitions [13], and produce rare-region phenomena [14]. In contrast to biological contagions, social contagions are strongly affected by social reinforcement [15]. Research on social contagions has focused primarily on a generalized Watts threshold model [16–21]. As in biological contagions, the behavior of NONs promotes social contagions [16]. Majdandzic *et al.* found multiple tipping points of social contagions in multilayer networks [21,22]. Recently Wang *et al.* used a data-driven asymmetric sociobiological coevolutionary model to locate an optimal information diffusion mechanism for suppressing biological contagions [23] that enables us to understand the effect of asymmetry in interacting dynamics [24–27].

Although there are many different communication channels, we usually select one to transmit information to friends during short periods of time due to the inelasticity of such resources as time and energy [28–30]. Thus when transmitting information through a multiplex network we often migrate to other channels [31,32], and a communication channel alteration (CCA) occurs. For example, when transmitting information using texting or email, if we change to another channel, then a CCA occurs. This event (i) creates distinct active time periods for individuals in different communication platforms and (ii) introduces time delays when obtaining information from other platforms. Theoretically CCA induces a non-Markovian effect into the spreading dynamics that further causes strong dynamic correlations among the states of neighbors.

---

*tangminghan007@gmail.com

Because there has been no systematic study of how CCA affects the dynamics of social contagions on multiplex networks, we propose a non-Markovian behavior spreading model on multiplex networks. At any given time an individual can be active in only one communication layer and can transmit behavioral information to neighbors and obtain behavioral information from neighbors only within the same subnetwork. Using extensive numerical simulations we find that time delays induced by CCA slow behavior spreading but do not affect the final adoption size. We also find that CCA suppresses the final behavior adoption size. It is significant that CCA changes the growth pattern of the final adoption size on Erdős-Rényi–Scale-Free (ER-SF) networks, i.e., the growth pattern of the adoption size versus the behavioral information transmission probability changes from continuous to hybrid. We develop a generalized edge-based compartmental method to describe this non-Markovian spreading model and find that the theoretical predictions agree with the numerical predictions.

II. SOCIAL CONTAGION MODEL ON MULTIPLEX NETWORKS

Communication channels such as Facebook, Twitter, and email facilitate interaction and information sharing. Taken together they form a multiplex network in which each communication channel functions as a subnetwork. During short periods of time individuals select a single communication platform to transmit information, and then CCA occurs. To understand how CCA affects the dynamics of social contagion, we examine the behavior spreading dynamics in two-layer multiplex networks in which each layer or subnetwork represents a single communication channel. Figure 1(a) shows a multiplex network. In the multiplex network model, subnetworks $\mathcal{A}$ and $\mathcal{B}$ have the same number of nodes, and they randomly match one to one, which means that each individual can communicate with friends through two different communication channels. To establish the multiplex network, we first assign degrees $k_{\mathcal{A}}$ and $k_{\mathcal{B}}$ to individuals in subnetworks $\mathcal{A}$ and $\mathcal{B}$, respectively, according to a joint degree distribution $P(\overrightarrow{K}) = P(k_{\mathcal{A}}, k_{\mathcal{B}})$. We then build each subnetwork using an uncorrelated configuration model [33]. In the thermodynamic limit, i.e., the network size $N \rightarrow \infty$, there are no intralayer degree correlations in the subnetworks.

We propose a generalized non-Markovian susceptible-adopted-recovered (SAR) model [34–36] to describe the behavior spreading dynamics in multiplex networks. Wang *et al.* [34] found a transition phenomenon in which the dependence of the final adoption size versus information transmission probability can change from discontinuous to continuous by decreasing the individual adoption threshold, increasing the initial seed size, or enhancing the network heterogeneity. In the SAR model, social reinforcement is triggered by the reception of nonredundant behavioral information, i.e., a susceptible individual adopts the new behavior only when the amount of received nonredundant information from neighbors rises above a given adoption threshold. We only allow the transmission of nonredundant information. An individual in the susceptible state has not adopted the behavior. An individual in the adopted state has adopted the behavior and is

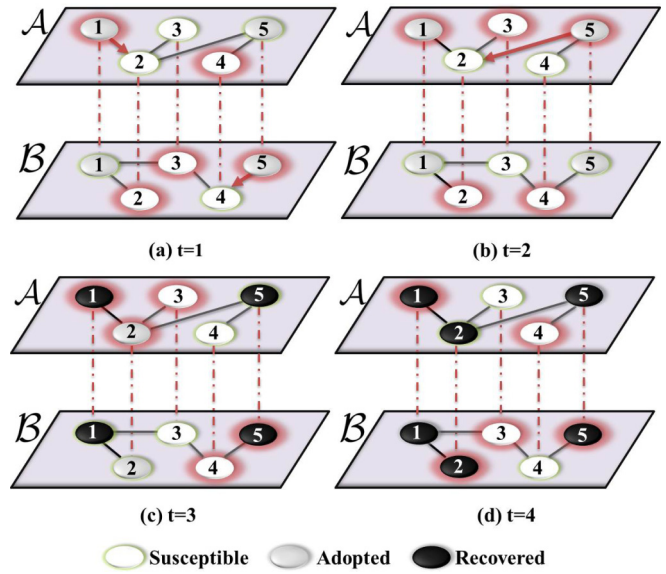
Susceptible ◯   **Adopted** ◯   **Recovered** ⬤

FIG. 1. Illustration of social contagions on multiplex networks. Initially, individuals 1 and 5 are selected as seeds (adopted), and the remaining individuals are susceptible. (a) At time $t = 1$, individual 1 (5) successfully transmits the information to his or her susceptible neighbor 2 (4) in subnetwork $\mathcal{A}$ ($\mathcal{B}$). The accumulated pieces of information of 2 (4) in subnetwork network $\mathcal{A}$ ($\mathcal{B}$) is $m_2^{\mathcal{A}} = 1$ ($m_4^{\mathcal{B}} = 1$). (b) At time $t = 2$, individuals 1, 3, and 5 are in subnetwork $\mathcal{A}$. Individual 5 successfully transmits the information to 2; however, individual 2 does not read this information since he or she belongs to subnetwork $\mathcal{B}$. (c) At $t = 3$, individual 2 activates in subnetwork $\mathcal{A}$, he or she fulfills his or her adoption threshold $T_{\mathcal{A}} = 2$. Thus, individual 2 adopts the behavior. Individuals 1 and 5 recover with probability $\gamma = 0.6$. (d) At time $t = 4$, all adopted individuals recover and no individual whose received information is greater than his or her adoption threshold. The processes terminates. Each individual activates in subnetwork $\mathcal{A}$ with probability $p = 0.6$ and in subnetwork $\mathcal{B}$ with the complementary probability $1 - p = 0.4$. Individuals activates in the subnetwork are marked with red shadow, such as individual 1 activates in $\mathcal{A}$.

willing to transmit the information to neighbors through one communication channel. An individual in the recovered state has lost interest in the behavior and no longer transmits the information.

During short periods of time the constraints posed by inelastic resources limit individuals to a single communication channel [28,29], i.e., at any given time step an individual can only be active in one subnetwork. Individuals thus use CCA as the system evolves. To describe CCA, we introduce a layer-switching parameter p_i and assume that individual i is active in subnetwork $\mathcal{A}$ with a probability p_i and active in subnetwork $\mathcal{B}$ with a probability $1 - p_i$. For simplicity, we assume that all individuals have equal values of $p = p_i$. When an individual is active in a subnetwork $\mathcal{X} \in \{\mathcal{A}, \mathcal{B}\}$, it can transmit the information to neighbors in subnetwork $\mathcal{X}$ and can read information from neighbors in subnetwork $\mathcal{X}$ but cannot read information in the other nonactive subnetwork $\mathcal{Y}$. Thus individuals cannot simultaneously read all information from neighbors in all communication channels, and this introduces *time delays* into receiving information.

We use a synchronous updating method [37] to renew the states of individuals. We first randomly select a fraction ρ_0 of individuals to be seeds in the adopted state. The remaining individuals are in the susceptible state. At each time step, each adopted individual $v_{\mathcal{X}}$ active in subnetwork $\mathcal{X}$ transmits the information to each susceptible neighbor $u_{\mathcal{X}}$ with a probability $\lambda_{\mathcal{X}}$. When individual $v_{\mathcal{X}}$ successfully transmits information to $u_{\mathcal{X}}$, the information transmission between them does not occur in subsequent steps, i.e., we only allow nonredundant information to transmit between two individuals because each neighbor can only partially guarantee the credibility and legitimacy of the behavior [38]. Note that if a susceptible individual $u_{\mathcal{X}}$ is active in subnetwork $\mathcal{X}$, he or she only reads information in subnetwork $\mathcal{X}$. Thus the CCA introduces time delays into receiving information. If an individual $u_{\mathcal{X}}$ in subnetwork $\mathcal{X}$ receives a new piece of information, he or she adopts the behavior with a probability $\pi(m_u^{\mathcal{A}}, m_u^{\mathcal{B}})$, where the $m_u^{\mathcal{X}}$ value is the number of cumulative pieces of nonredundant information from neighbors in subnetwork $\mathcal{X}$. If individual $u_{\mathcal{X}}$ adopts the behavior, then his or her counterpart $u_{\mathcal{Y}}$ also adopts the behavior in subnetwork $\mathcal{Y}$. Here we focus on a case in which an individual in the susceptible state adopts the new behavior when $m_u^{\mathcal{X}}$ exceeds his or her adoption threshold $T_u^{\mathcal{X}}$ in subnetwork $\mathcal{X}$. For simplicity, we assume all individuals have the same adoption threshold $T_u^{\mathcal{X}} = T_{\mathcal{X}}$ in subnetwork $\mathcal{X}$. The $\pi(m_u^{\mathcal{A}}, m_u^{\mathcal{B}})$ value is

$$\pi\left(m_u^{\mathcal{A}}, m_u^{\mathcal{B}}\right) = \begin{cases} 1, & m_u^{\mathcal{A}} \geqslant T_{\mathcal{A}} \text{ or } m_u^{\mathcal{B}} \geqslant T_{\mathcal{B}} \\ 0, & \text{others} \end{cases}. \quad (1)$$

To include the social reinforcement effect, both $T_{\mathcal{A}}$ and $T_{\mathcal{B}}$ values are greater than unity. At each time step we assume that all individuals in the adopted state lose interest in transmitting the information and with a probability γ they recover. The spreading stops when all the adopted individuals become recovered, and the received information of all susceptible individuals does not exceed their threshold in either subnetwork. Figure 1 shows the behavior spreading dynamics in multiplex networks.

There are two key features in our proposed spreading dynamics. (1) The memory effect is induced in our model. Unlike bootstrap percolation [39–41] or a threshold model [19] in which a susceptible individual becomes active (or adopted) only when its current number or fraction of adopted neighbors is larger than a given value, in our model a susceptible individual becomes adopted when his or her received accumulated information in either subnetwork is larger than a threshold. (2) CCA is included in our model. Unlike the models in Refs. [16,18] in which each node can obtain the information from two subnetworks simultaneously, CCA allows an individual to be active in only one subnetwork at a time step.

III. THEORETICAL METHOD

From the description of the behavior adoption process in Sec. II we know that there is a *non-Markovian* characteristic in the dynamics because (i) social reinforcement occurs when nonredundant behavioral information transmissions are remembered, and (ii) CCA causes time delays in the reception of information. This non-Markovian characteristic makes the
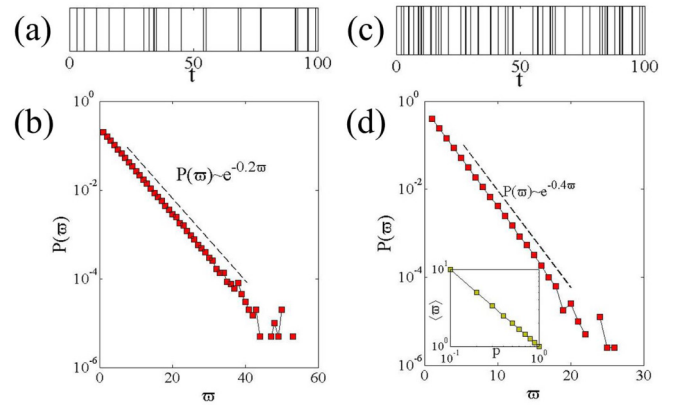

FIG. 2. Dynamics of social contagions on RR-RR multiplex networks. Active events in subnetwork $\mathcal{A}$, i.e., individuals are active in subnetwork $\mathcal{A}$, versus time ϖ with (a) $p = 0.8$ and (c) $p = 0.6$, respectively. The time interval distribution $P(\varpi)$ between two consecutive activates in subnetwork $\mathcal{A}$ with (b) $p = 0.8$ and (d) $p = 0.6$, respectively. We set other parameters to be $\rho_0 = 0.1$, $\gamma = 1.0$, $k = 10$, $\lambda_{\mathcal{A}} = \lambda_{\mathcal{B}} = 0.9$, and $T_{\mathcal{A}} = T_{\mathcal{A}} = 3$.

strong dynamic correlations among the states of the neighbors difficult to describe. Here we develop a generalized edge-based compartmental method [42–45] of describing the spreading of behavior in multiplex networks. In this theoretical method we assume that the networks are large, the edges sparse, there are no degree-degree correlations, and the dynamics evolve continuously.

An individual u adopting the new behavior must take into account his or her received information in both subnetworks $\mathcal{A}$ and $\mathcal{B}$. Denoting $u_{\mathcal{X}}$ as an individual u active in subnetwork $\mathcal{X} \in \{\mathcal{A}, \mathcal{B}\}$, we quantify the probability that individual u is in the susceptible state and assume that $u_{\mathcal{X}}$ is in the cavity state [46], i.e., that $u_{\mathcal{X}}$ cannot transmit the information to neighbors in subnetwork $\mathcal{X}$ but can receive information from neighbors in all the subnetworks. The probability that an individual $v_{\mathcal{X}}$ has not transmitted the information to a neighbor $u_{\mathcal{X}}$ along a randomly chosen edge in subnetwork $\mathcal{X}$ by time t is $\theta_{\mathcal{X}}(t)$. At time t, the probability that $u_{\mathcal{X}}$ has received units of information $m_{\mathcal{X}}$ from subnetwork $\mathcal{X}$ is

$$\phi_{m_{\mathcal{X}}}^{\mathcal{X}}(k_{\mathcal{X}}, t) = \binom{k_{\mathcal{X}}}{m_{\mathcal{X}}}[\theta_{\mathcal{X}}(t)]^{k_{\mathcal{X}} - m_{\mathcal{X}}}[1 - \theta_{\mathcal{X}}(t)]^{m_{\mathcal{X}}}, \quad (2)$$

where $k_{\mathcal{X}}$ is the degree of individual u in subnetwork $\mathcal{X}$. Here the CCA disallows individual $u_{\mathcal{X}}$ from reading all information from all subnetworks because he or she can only focus on the information in the layer in which he or she is currently active. At time t, individual u can only read received information from neighbors in subnetwork $\mathcal{X}$ when he or she is active in that subnetwork, i.e., when u is active in $\mathcal{X}$ he or she cannot read received information in $\mathcal{Y}$.

The CCA between two subnetworks for individual u is a stochastic Poisson process. The time interval distribution between two successive actions of u in subnetwork $\mathcal{A}$ is $P(\overline{\omega}) \sim e^{-(1-p)\overline{\omega}}$ [47], as shown in Figs. 2(a) and 2(b) and Figs. 2(d) and 2(e), where p is the probability that u is active in subnetwork $\mathcal{A}$. Note that we use random regular (RR) [48] networks to describe the two subnetworks $\mathcal{A}$ and

$\mathcal{B}$ in Fig. 2. All nodes have the same degree in the RR network, i.e., $P_{\mathcal{A}}(k_{\mathcal{A}}) = P_{\mathcal{B}}(k_{\mathcal{B}}) = 1$ if $\langle k_{\mathcal{A}} \rangle = \langle k_{\mathcal{B}} \rangle = 10$. Each RR network can be built using an uncorrelated configuration model [33]. We find the approximate average time interval of all individuals active in subnetwork $\mathcal{X}$ to be

$$\langle \overline{\omega}_{\mathcal{X}} \rangle = \frac{1}{1 - p_{\mathcal{X}}}, \tag{3}$$

where $p_{\mathcal{X}}$ is the probability that an individual is active in subnetwork $\mathcal{X}$. When $\mathcal{X} = \mathcal{A}$, then $p_{\mathcal{X}} = p$. When $\mathcal{X} = \mathcal{B}$, then $p_{\mathcal{X}} = 1 - p$.

If individual u is active in subnetwork $\mathcal{Y}$ at time t, on average his or her latest active time in subnetwork $\mathcal{X}$ is $t - \langle \overline{\omega}_{\mathcal{X}} \rangle$. Here he or she reads all information in subnetwork $\mathcal{Y}$. The approximate number of information units he can read in subnetwork $\mathcal{X}$ is the number of information units in the inbox of subnetwork $\mathcal{X}$ at $t - \langle \overline{\omega}_{\mathcal{X}} \rangle$. The cumulative number of information units $n_{\mathcal{X}}$ read by susceptible individual $u_{\mathcal{X}}$ at time t has a probability

$$\chi_{n_{\mathcal{X}}}^{\mathcal{X}}(k_{\mathcal{X}}, t) = \binom{k_{\mathcal{X}}}{n_{\mathcal{X}}} [\theta_{\mathcal{X}}(t - \langle \overline{\omega}_{\mathcal{X}} \rangle)]^{k_{\mathcal{X}} - n_{\mathcal{X}}}$$
$$\times [1 - \theta_{\mathcal{X}}(t - \langle \overline{\omega}_{\mathcal{X}} \rangle)]^{n_{\mathcal{X}}}. \tag{4}$$

If individual u with degree $\overrightarrow{K} = (k_{\mathcal{A}}, k_{\mathcal{B}})$ has not adopted the behavior by time t, then the cumulative pieces of information individual u has read in both subnetworks $\mathcal{A}$ and $\mathcal{B}$ will be less than the adoption thresholds $T_{\mathcal{A}}$ and $T_{\mathcal{B}}$, respectively. At time t, if individual u is active in subnetwork $\mathcal{A}$, then he or she remains susceptible with a probability

$$F_{\mathcal{A}}(\overrightarrow{K}, t) = \sum_{m_{\mathcal{A}}=0}^{k_{\mathcal{A}}} \sum_{n_{\mathcal{B}}=0}^{k_{\mathcal{B}}} \phi_{m_{\mathcal{A}}}^{\mathcal{A}}(k_{\mathcal{A}}, t) \chi_{n_{\mathcal{B}}}^{\mathcal{B}}(k_{\mathcal{B}}, t)$$
$$\times \prod_{j_{\mathcal{A}}=0}^{m_{\mathcal{A}}} \prod_{j_{\mathcal{B}}=0}^{n_{\mathcal{B}}} [1 - \pi(j_{\mathcal{A}}, j_{\mathcal{B}})]. \tag{5}$$

Similarly, if individual u is active in subnetwork $\mathcal{B}$ at time t, then he or she remains susceptible with a probability

$$F_{\mathcal{B}}(\overrightarrow{K}, t) = \sum_{n_{\mathcal{A}}=0}^{k_{\mathcal{A}}} \sum_{m_{\mathcal{B}}=0}^{k_{\mathcal{B}}} \chi_{n_{\mathcal{A}}}^{A}(k_{\mathcal{A}}, t) \phi_{m_{\mathcal{B}}}^{\mathcal{B}}(k_{\mathcal{B}}, t)$$
$$\times \prod_{j_{\mathcal{A}}=0}^{n_{\mathcal{A}}} \prod_{j_{\mathcal{B}}=0}^{m_{\mathcal{B}}} [1 - \pi(j_{\mathcal{A}}, j_{\mathcal{B}})]. \tag{6}$$

The probability that individual u with a degree $\overrightarrow{K}$ is susceptible is

$$s(\overrightarrow{K}, t) = (1 - \rho_0)[p_{\mathcal{A}} F_{\mathcal{A}}(\overrightarrow{K}, t) + p_{\mathcal{B}} F_{\mathcal{B}}(\overrightarrow{K}, t)], \tag{7}$$

where the factor $(1 - \rho_0)$ is the probability that individual u is initially susceptible, and $p_{\mathcal{X}} = \frac{1}{N} \sum_{u=1}^{N} p_u^{\mathcal{X}}$ is the average probability that individual u is active in subnetwork $\mathcal{X}$. Note that $p_{\mathcal{A}} = 1 - p_{\mathcal{B}}$. Examining the degree distribution $P(\overrightarrow{K})$, the fraction of susceptible individuals at time t is

$$S(t) = \sum_{\overrightarrow{K}} P(\overrightarrow{K}) s(\overrightarrow{K}, t). \tag{8}$$

According to the definition of $\theta_{\mathcal{X}}$, an endpoint individual $v_{\mathcal{X}}$ of the randomly selected edge of $u_{\mathcal{X}}$ can be in a susceptible, adopted, or recovered state, and thus $\theta_{\mathcal{X}}(t)$ can be rewritten

$$\theta_{\mathcal{X}}(t) = \xi_S^{\mathcal{X}}(t) + \xi_A^{\mathcal{X}}(t) + \xi_R^{\mathcal{X}}(t), \tag{9}$$

where $\xi_S^{\mathcal{X}}(t)$ [$\xi_A^{\mathcal{X}}(t)$ or $\xi_R^{\mathcal{X}}(t)$] is the probability that individual $v_{\mathcal{X}}$ is susceptible (adopted or recovered) and has not transmitted the information to $u_{\mathcal{X}}$ by time t.

If individual $u_{\mathcal{X}}$ is initially susceptible, then he or she is in the cavity state and thus cannot transmit the information to susceptible neighbors $v_{\mathcal{X}}$ in subnetworks $\mathcal{X}$. When individual $v_{\mathcal{X}}$ with degree $k'_{\mathcal{X}}$ is susceptible and active in subnetwork $\mathcal{X}$, he or she can only receive the information from $k'_{\mathcal{X}} - 1$ other neighbors in subnetwork $\mathcal{X}$. At time t, if the susceptible individual $v_{\mathcal{X}}$ is active in subnetwork $\mathcal{X}$, then the probability that he can read $m_{\mathcal{X}}$ pieces of information from this subnetwork is

$$\tau_{m_{\mathcal{X}}}^{\mathcal{X}}(k'_{\mathcal{X}}, t) = \binom{k'_{\mathcal{X}} - 1}{m_{\mathcal{X}}} \theta_{\mathcal{X}}(t)^{k'_{\mathcal{X}} - m_{\mathcal{X}} - 1} [1 - \theta_{\mathcal{X}}(t)]^{m_{\mathcal{X}}}. \tag{10}$$

In contrast, individual v can only read the information at time $t - \langle \overline{\omega}_{\mathcal{X}} \rangle$ in subnetwork $\mathcal{X}$ when he or she is active in subnetwork $\mathcal{Y}$ at time t. As in Eq. (4), the probability that individual $v_{\mathcal{X}}$ reads $n_{\mathcal{X}}$ pieces of information is

$$\varsigma_{n_{\mathcal{X}}}^{\mathcal{X}}(k'_{\mathcal{X}}, t) = \binom{k'_{\mathcal{X}} - 1}{n_{\mathcal{X}}} \theta_{\mathcal{X}}(t - \langle \overline{\omega}_{\mathcal{X}} \rangle)^{k'_{\mathcal{X}} - n_{\mathcal{X}} - 1}$$
$$\times [1 - \theta_{\mathcal{X}}(t - \langle \overline{\omega}_{\mathcal{X}} \rangle)]^{n_{\mathcal{X}}}. \tag{11}$$

Individual $v_{\mathcal{X}}$ remains susceptible when the cumulative pieces of information read from neighbors in subnetwork $\mathcal{X}$ is lower than adoption threshold $T_{\mathcal{X}}$ in the absence of individual $u_{\mathcal{X}}$. When v is active in subnetwork $\mathcal{X}$, he or she reads $n_{\mathcal{Y}}$ pieces of information in subnetwork $\mathcal{Y}$ with a probability $\chi_{n_{\mathcal{Y}}}^{\mathcal{Y}}(k'_{\mathcal{Y}}, t)$ [see Eq. (4)]. Thus the probability that individual v is susceptible is

$$\Psi_{\mathcal{X}}^{\mathcal{X}}(\overrightarrow{K}, t) = \sum_{m'_{\mathcal{X}}=0}^{k'_{\mathcal{X}}-1} \sum_{n'_{\mathcal{Y}}=0}^{k'_{\mathcal{Y}}} \tau_{m'_{\mathcal{X}}}^{\mathcal{X}}(k'_{\mathcal{X}}, t) \chi_{n'_{\mathcal{Y}}}^{\mathcal{Y}}(k'_{\mathcal{Y}}, t)$$
$$\times \prod_{j'_{\mathcal{X}}=0}^{m'_{\mathcal{X}}} \prod_{j'_{\mathcal{Y}}=0}^{n'_{\mathcal{Y}}} [1 - \pi(j'_{\mathcal{X}}, j'_{\mathcal{Y}})]. \tag{12}$$

Similarly, when individual v is active in subnetwork $\mathcal{Y}$ the probability that v will read $n_{\mathcal{X}}$ and $m_{\mathcal{Y}}$ pieces of information from subnetworks $\mathcal{X}$ and $\mathcal{Y}$ is $\varsigma_{n_{\mathcal{X}}}^{\mathcal{X}}(k'_{\mathcal{X}}, t)$ and $\phi_{m_{\mathcal{Y}}}^{\mathcal{Y}}(k'_{\mathcal{Y}}, t)$, respectively. The probability that individual v is susceptible is

$$\Psi_{\mathcal{X}}^{\mathcal{Y}}(\overrightarrow{K}, t) = \sum_{n'_{\mathcal{X}}=0}^{k'_{\mathcal{X}}-1} \sum_{m'_{\mathcal{Y}}=0}^{k'_{\mathcal{Y}}} \varsigma_{n'_{\mathcal{X}}}^{\mathcal{X}}(k'_{\mathcal{X}}, t) \phi_{m'_{\mathcal{Y}}}^{\mathcal{Y}}(k'_{\mathcal{Y}}, t)$$
$$\times \prod_{j'_{\mathcal{X}}=0}^{n'_{\mathcal{X}}} \prod_{j'_{\mathcal{Y}}=0}^{m'_{\mathcal{Y}}} [1 - \pi(j'_{\mathcal{X}}, j'_{\mathcal{Y}})]. \tag{13}$$

When an initially susceptible individual v is active in subnetwork $\mathcal{X}$, the probability that he or she remains susceptible is

$$\Theta_{\mathcal{X}}(\overrightarrow{K}, t) = p_{\mathcal{X}} \Psi_{\mathcal{X}}^{\mathcal{X}}(\overrightarrow{K}, t) + p_{\mathcal{Y}} \Psi_{\mathcal{X}}^{\mathcal{Y}}(\overrightarrow{K}, t). \tag{14}$$

Denoting $H_{\mathcal{X}}(k'_{\mathcal{X}} | k_{\mathcal{X}})$ to be the probability of a node with degree $k_{\mathcal{X}}$ connects to a node with degree $k'_{\mathcal{X}}$ in network

$\mathcal{X}$. Thus the probability that individual $u_\mathcal{X}$ connects to a susceptible individual in subnetwork $\mathcal{X}$ is

$$\xi_S^\mathcal{X}(t) = (1 - \rho_0) \sum_{\vec{K}} H_\mathcal{X}(k'_\mathcal{X}|k_\mathcal{X}) \Theta_\mathcal{X}(\vec{K}, t). \quad (15)$$

In an uncorrelated network, $H_\mathcal{X}(k'_\mathcal{X}|k_\mathcal{X}) = k'_\mathcal{X} P(\vec{K})/\langle k_\mathcal{X} \rangle$. We rewrite Eq. (15) to be

$$\xi_S^\mathcal{X}(t) = (1 - \rho_0) \frac{1}{\langle k_\mathcal{X} \rangle} \sum_{\vec{K}} k'_\mathcal{X} P(\vec{K}) \Theta_\mathcal{X}(\vec{K}, t). \quad (16)$$

When the information transmits through an edge at time t in subnetwork $\mathcal{X}$, the edge does not fulfill the definition of $\theta_\mathcal{X}(t)$. The decreasing of $\theta_\mathcal{X}(t)$ is thus

$$\frac{d\theta_\mathcal{X}(t)}{dt} = -p_\mathcal{X} \lambda_\mathcal{X} \xi_A^\mathcal{X}(t). \quad (17)$$

For $\xi_R^\mathcal{X}(t)$ to grow, (i) the information cannot be transmitted through the edge and (ii) the adopted individual must recover at time t. The evolution of $\xi_R^\mathcal{X}(t)$ is

$$\frac{d\xi_R^\mathcal{X}(t)}{dt} = \gamma(1 - p_\mathcal{X} \lambda_\mathcal{X}) \xi_A^\mathcal{X}(t). \quad (18)$$

Combining Eqs. (17) and (18) and the initial condition $\theta_\mathcal{X}(0) = 1$ and $\xi_R^\mathcal{X}(0) = 0$ gives us

$$\xi_R^\mathcal{X}(t) = \frac{\gamma(1 - p_\mathcal{X} \lambda_\mathcal{X})[1 - \theta_\mathcal{X}(t)]}{p_\mathcal{X} \lambda_\mathcal{X}}. \quad (19)$$

We use Eqs. (9), (16), (17), and (19) to obtain the value of $\theta_\mathcal{X}(t)$.

Using the evolution process of the behavior spreading dynamics described in Sec. II, we derive the evolution equations of the fraction of individuals in the adopted and recovered states,

$$\frac{dA(t)}{dt} = -\frac{dS(t)}{dt} - \gamma A(t) \quad (20)$$

and

$$\frac{dR(t)}{dt} = \gamma A(t), \quad (21)$$

respectively. Combining Eqs. (8) and (20)–(21), we obtain the time evolution of the behavior spreading dynamics in multiplex networks. When $t \to \infty$, the final behavior adoption size is denoted $R(\infty)$.

We next examine the growth pattern of the final behavior adoption size $R(\infty)$ versus the information transmission probability $\vec{\lambda} = (\lambda_\mathcal{A}, \lambda_\mathcal{B})$ and the CCA probability p. We first investigate the effects of the time delays induced by CCA on the dynamics of social contagions by comparing them with a null model without time delays. Details about the null model are supplied in the Appendix. Figure 3(a) shows that the time delays–induced CCA affect behavior spreading dynamics, including the time evolutions of susceptible $S(t)$, adopted $A(t)$, and recovered $R(t)$ individuals. We find that $S(t)[R(t)]$ decreases (increases) with t and that $A(t)$ first increases and then decreases. Note that the time delays induced by CCA slow behavior adoption. To quantify the slowing caused by the time delays induced by CCA, we compute the stabilizing time of the system $t_{\max}$, i.e., the average time needed for the
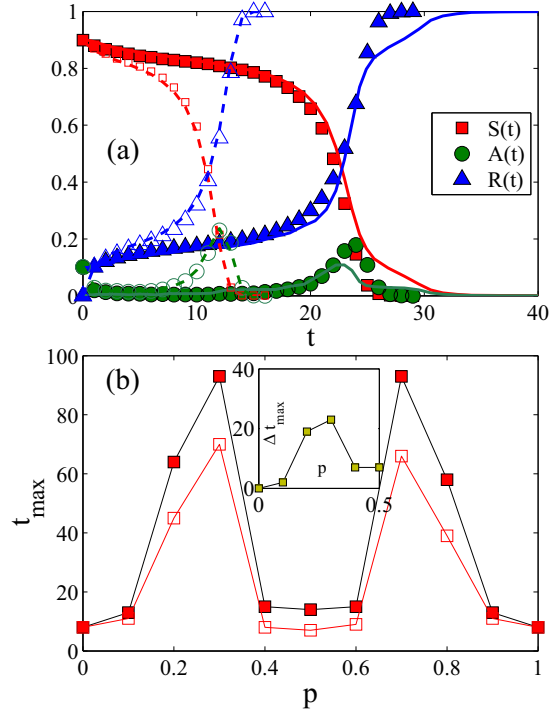

FIG. 3. Dynamics of social contagions on RR-RR multiplex networks. (a) The time evolutions of susceptible $S(t)$, adopted $A(t)$, and recovered $R(t)$ individuals with (solid symbols) and without (empty symbols) time delays when $p = 0.8$. The symbols are numerical simulation results and lines are the theoretical predictions. (b) The stabilizing time of the system $t_{\max}$ with (solid symbols) and without (empty symbols) time delays versus p. The inset of (b) shows the retardation time as a function of p for the system with or without time delays. We set other parameters to be $\rho_0 = 0.1$, $\gamma = 1.0$, $k = 10$, $\lambda_\mathcal{A} = \lambda_\mathcal{B} = 0.9$, and $T_\mathcal{A} = T_\mathcal{A} = 3$.

system to reach the final state. When $0 \leqslant p \leqslant 0.5$, $t_{\max}$ first increases with p and then decreases. When the p value is small, most individuals are active in subnetwork $\mathcal{B}$. When susceptible individuals receive information that exceeds his or her adoption threshold, they quickly adopt the behavior. When the p value is increased, some individuals become active in subnetwork $\mathcal{A}$ but adopt the behavior only after their received information exceeds their adoption threshold. Thus $t_{\max}$ first increases. When the p value is large, fewer individuals adopt the behavior (see Fig. 4) and $t_{\max}$ thus decreases. The inset of Fig. 3(b) shows the retardation time $\Delta t_{\max}$ for social contagion models with and without time delays. Note that $\Delta t_{\max}$ first increases with p and then decreases. We find the same phenomena for $0.5 \leqslant p \leqslant 1.0$ because subnetworks $\mathcal{A}$ and $\mathcal{B}$ are both RR networks.

Figure 3(a) shows that the time delays induced by CCA do not affect the final behavior adoption size $R(\infty)$. This is because when a susceptible individual fulfills the behavior adoption conditions the time delays affect only the behavior adoption time. This also indicates that the critical points of the system remain the same when there are no time delays in his or her behavior adoption, i.e., a susceptible individual adopts the new behavior as soon as the received pieces of information equal or exceed the adoption threshold, independent of the
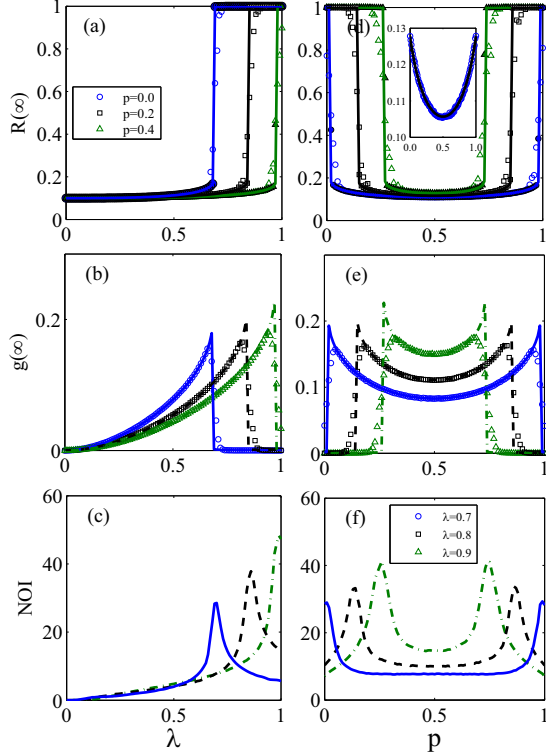
FIG. 4. Behavior spreading on RR-RR networks. (a) Final behavior adoption size $R(\infty)$, (b) the fraction of individuals in the subcritical state $g(\infty)$, and (c) NOI versus information transmission probability λ for CCA probability $p = 0.0$, 0.2, and 0.4. (d) $R(\infty)$, (e) $g(\infty)$, and (f) NOI versus p for $\lambda = 0.7$, 0.8, and 0.9. The inset of (d) shows $R(\infty)$ versus p for $\lambda = 0.6$. The empty (full) symbols are the simulated values of $R(\infty)$ at network size $N = 10^4$ ($N = 10^6$). The lines in (a), (b), (d), and (e) are the theoretical values and are numerical simulation results in (c) and (f). Other parameters are $\rho_0 = 0.1$, $\gamma = 1.0$, $\langle k \rangle = 10$, and $T_\mathcal{A} = T_\mathcal{A} = 3$, respectively.

subnetwork in which he or she is currently active. Thus when examining the final state of the behavior we disregard time delays, i.e., Eqs. (4) and (11) are the same as Eqs. (2) and (10), respectively. We perform numerical simulations and theoretical analyses of the social contagions on ER-SF multiplex networks and find that the time delays induced by CCA slow the spreading dynamics but do not affect the final adoption size.

In the final state, i.e., when $t \to \infty$, there are no nodes in the adopted state, and no information is transmitted through edges. Thus we have $d\theta_\mathcal{X}(t)/dt = 0$ and $\theta_\mathcal{X}(t) = \theta_\mathcal{X}(t - \langle \overline{\omega}_\mathcal{X} \rangle) = \theta_\mathcal{X}^*$. Combining Eqs. (9), (16)–(17), and (19) we obtain

$$
\theta_\mathcal{X}^* = (1 - \rho_0) \frac{\sum_{\overrightarrow{K}} k_\mathcal{X} P(\overrightarrow{K}) \Theta_\mathcal{X}(\overrightarrow{K}, \infty)}{\langle k_\mathcal{X} \rangle}
$$

$$
+ \frac{\gamma(1 - p_\mathcal{X} \lambda_\mathcal{X})[1 - \theta_\mathcal{X}^*]}{p_\mathcal{X} \lambda_\mathcal{X}}
$$

$$
= f_\mathcal{X}(\theta_\mathcal{A}^*, \theta_\mathcal{B}^*). \tag{22}
$$

When $\rho_0 \to 0$, then $\theta_\mathcal{X}^* = 1$ is a trivial solution of Eq. (22), but this vanishingly small fraction of seeds cannot trigger

global behavior adoption because $T_\mathcal{X} > 1$ [34]. To stimulate global behavior adoption, we must have a finite fraction of seed individuals. Here $\theta_\mathcal{X}^* = 1$ is no longer the solution of Eq. (22), which now has either one or three fixed points (including multiplicity). If Eq. (22) has only one solution at all values of $\lambda_\mathcal{X}$, then $\theta_\mathcal{X}^*$ decreases continuously with $\lambda_\mathcal{X}$, and this leads to a continuous growth pattern in the final behavior adoption $R(\infty)$. If the number of the solutions of Eq. (22) varies with $\lambda_\mathcal{X}$, then the situation is different. For a given $\lambda_\mathcal{X}$, if there is only one fixed point of Eq. (22), then it is the physically meaningful solution. If there are three fixed points, which are stable, unstable, and saddle points, then only the maximum solution is physically meaningful in our irreversible behavior spreading dynamics when we randomly select a relatively small fraction of seeds, since the individuals in the adopted state persistently transmit the information to their neighbors, and $\theta_\mathcal{X}^*$ decreases from unity. Thus a saddle-node bifurcation occurs [49,50]. Through a bifurcation analysis of Eq. (22), we find that the system undergoes a cusp catastrophe: Varying $\lambda_\mathcal{X}$ the physically meaningful stable solution of $\theta_\mathcal{X}^*$ suddenly produces a different outcome. Therefore, the growth patten of $R(\infty)$ will be discontinuous because a meaningful solution decreases abruptly at such critical conditions as the critical information transmission probability $\overrightarrow{\lambda}_c$ and the critical CCA probability p_c.

To determine p_c, we first rewrite Eq. (22) to be

$$
F_\mathcal{A}(\theta_\mathcal{A}^*, \theta_\mathcal{B}^*) = \theta_\mathcal{A}^* - f_\mathcal{A}(\theta_\mathcal{A}^*, \theta_\mathcal{B}^*) = 0 \tag{23}
$$

and

$$
F_\mathcal{B}(\theta_\mathcal{A}^*, \theta_\mathcal{B}^*) = \theta_\mathcal{B}^* - f_\mathcal{B}(\theta_\mathcal{A}^*, \theta_\mathcal{B}^*) = 0. \tag{24}
$$

At the discontinuous critical point, the curves of $f_\mathcal{A}(\theta_\mathcal{A}^*, \theta_\mathcal{B}^*)$ and $f_\mathcal{B}(\theta_\mathcal{A}^*, \theta_\mathcal{B}^*)$ are tangent to each other at the discontinuous critical point [51,52]. Thus we find that the critical point for the discontinuous growth pattern is given by $\frac{d\theta_\mathcal{A}^*(\theta_\mathcal{B}^*)}{d\theta_\mathcal{B}^*} \frac{d\theta_\mathcal{B}^*(\theta_\mathcal{A}^*)}{d\theta_\mathcal{A}^*} = 1$. Combining Eqs. (23) and (24), we further obtain the discontinuous critical points of $\overrightarrow{\lambda}_c$ and p_c by solving both Eq. (22) and

$$
\frac{\partial f_\mathcal{A}(\theta_\mathcal{A}^*, \theta_\mathcal{B}^*)}{\partial \theta_\mathcal{B}^*} \frac{\partial f_\mathcal{B}(\theta_\mathcal{A}^*, \theta_\mathcal{B}^*)}{\partial \theta_\mathcal{A}^*} = 1. \tag{25}
$$

IV. NUMERICAL SIMULATIONS

Here we perform extensive simulations on multiplex networks, including RR-RR networks (i.e., in which each subnetwork is a RR network) and ER-SF networks (i.e., in which subnetworks $\mathcal{A}$ and $\mathcal{B}$ are ER [53] and SF [33] networks, respectively). In each case we set the network size, average degree, and recovery probability to be $N = 10^4$, $\rho_0 = 0.1$, $\langle k_\mathcal{A} \rangle = \langle k_\mathcal{B} \rangle = 10$, and $\gamma = 1.0$, respectively, unless stated otherwise.

A. RR-RR multiplex networks

We first study social contagions on RR-RR multiplex networks in which each node in each subnetwork has a degree $k = 10$. Figure 4(a) shows $R(\infty)$ as a function of λ under different CCA probabilities p. We find that $R(\infty)$ first grows continuously for small values of λ and then increases

discontinuously at λ_c, i.e., exhibiting a hybrid growth, regardless of p. We can understand the discontinuous increasing of $R(\infty)$ by studying the fraction of individuals $g(\infty)$ in the subcritical state. When an individual is in the subcritical state he has received the information but have not adopted the behavior, and the number of information units from distinct neighbors is one less than the adoption threshold in subnetwork $\mathcal{A}$ or $\mathcal{B}$ [34]. Slightly increasing the value of λ can increase the number of subcritical state individuals with information units equal to or greater than their threshold [see Fig. 4(b)] and lead to a discontinuous jump in $R(\infty)$. In addition, $R(\infty)$ decreases with p, since an increasing number of susceptible individuals are unable to fulfill the behavior adoption condition. Because near the critical point the system exhibits a critical slowing, we locate the numerical critical point λ_c^1 by examining the number of iterations (NOI), which is widely used in the bootstrap percolation [39–41] and cascading failures [54,55], required to reach the final state, and we take into account only iterations in which at least one individual adopts the behavior. Figure 4(c) shows that at the critical point the NOI exhibit a peak. Note that our theoretical method accurately predicts $R(\infty)$ and the growth pattern of $R(\infty)$. The deviations around the critical points are caused by finite-size network effects [see Fig. 4(a)].

Figures 4(d)–4(f) show the effect of p on social contagions. Unlike when $T_\mathcal{A} = T_\mathcal{B} = 1$ in Fig. 7 of Appendix B, Fig. 4(d) shows that the final behavior adoption size $R(\infty)$ versus p is nonmonotonic. Specifically, for relatively small values of $\lambda = 0.6$ few susceptible individuals adopt the behavior, and $R(\infty)$ first decreases *continuously* with p and then increases *continuously* [see the inset in Fig. 4(d)]. For large values of $\lambda = 0.7, 0.8, 0.9$, $R(\infty)$ first decreases *discontinuously* with p and then increases *discontinuously* [see Fig. 4(d)]. We can similarly understand the growth pattern of $R(\infty)$ by studying $g(\infty)$. For a small value of p, e.g., $p = 0.1$ when $\lambda = 0.9$, most individuals in subnetwork $\mathcal{A}$ are active, many individuals adopt the behavior, and few individuals remain in the subcritical state [see Fig. 4(e)]. With an increase of p, fewer individuals are active in subnetwork $\mathcal{B}$, many individuals in subnetwork $\mathcal{A}$ are in the subcritical state [see Fig. 4(e)], and there is a sharp decrease in $R(\infty)$. By further increasing p, many individuals "jump" between subnetworks $\mathcal{A}$ and $\mathcal{B}$, and fewer individuals receive one fewer information units than the adoption threshold in the two subnetworks. Thus $g(\infty)$ decreases [see Fig. 4(e)]. Similarly, $g(\infty)$ first increases and then decreases discontinuously when the value of p is large. Note that NOI versus p exhibits two peaks at $p_c^1 = 1 - p_c^2$ because the two subnetworks are RR networks [see Fig. 4(f)].

B. ER-SF multiplex networks

When studying social contagions on ER-SF multiplex networks, we assume that there are no degree-degree correlations in the intralayers and interlayers. We generate the SF networks using the same method as that used in uncorrelated configuration networks that have a power-low degree distribution $P_\mathcal{B}(k_\mathcal{B}) = \frac{1}{\sum_{k_\mathcal{B}} k_\mathcal{B}^{-\upsilon_\mathcal{B}}} k_\mathcal{B}^{-\upsilon_\mathcal{B}}$. In network $\mathcal{B}$ without degree-degree correlations, the maximum degree follows a structural cutoff [56], i.e., $k_{\max} \sim \sqrt{N}$. The SF network is built using the uncorrelated configuration method in Ref. [33]. Figure 5
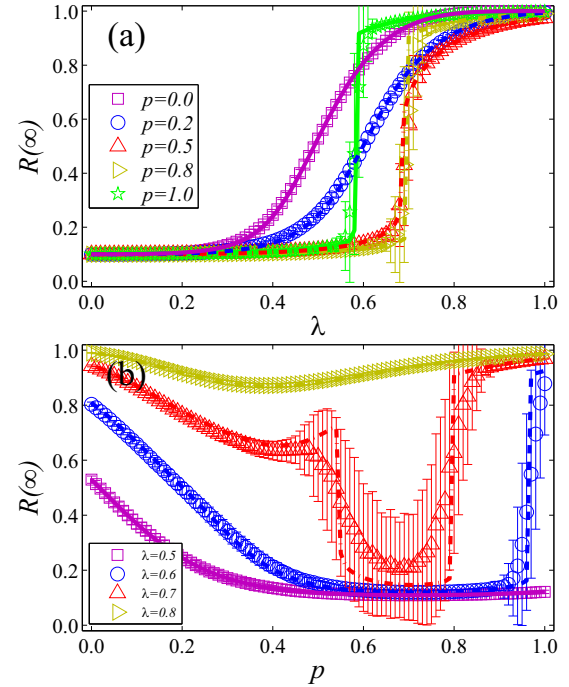

FIG. 5. Dynamics of social contagions on uncorrelated ER-SF multiplex networks. (a) The final behavior adoption size $R(\infty)$ versus information transmission probability λ under different communication channels alternation probability p. (b) $R(\infty)$ as a function of p for different λ. Lines are the theoretical predictions from Eqs. (7) and (17)–(19). The error bars indicate the standard deviations. Other parameters are set to be $\langle k_\mathcal{A} \rangle = 10$, $\langle k_\mathcal{B} \rangle = 10$, $\upsilon_\mathcal{B} = 3.0$, $\rho_0 = 0.1$, and $T_\mathcal{A} = T_\mathcal{A} = 3$.

shows the social contagions on ER-SF networks. Figure 5(a) shows that CCA changes the growth pattern of $R(\infty)$ versus λ. When $p = 0.0$ (1.0), the number of individuals only active in subnetwork $\mathcal{B}$ ($\mathcal{A}$) and $R(\infty)$ grows continuously (discontinuously) versus λ (see Ref. [34]). Increasing p increases the number of individuals active in the homogeneous subnetwork $\mathcal{A}$, and there are more individuals in the subcritical state who are likely to simultaneously adopt the behavior. Thus we see a hybrid growth in $R(\infty)$, i.e., $R(\infty)$ first grows continuously for small values of λ, and then grows discontinuously at λ_c.

Figure 5(b) shows that $R(\infty)$ versus p exhibits differing patterns under different values of λ. For a small value $\lambda = 0.5$, $R(\infty)$ first decreases continuously with p. For a relatively large value, e.g., $\lambda = 0.6$, $R(\infty)$ first decreases continuously with p and then increases discontinuously. Note that when $\lambda = 0.7$, $R(\infty)$ first decreases continuously with p and then increases to a peak at some p, then decreases discontinuously and, finally, increases discontinuously. For a very large value $\lambda = 0.9$, $R(\infty)$ first decreases continuously and then increases continuously. For intermediate values of $0 < p < 1$, the CCA emerges and constrains user ability to receive enough information to exceed the adoption threshold of a subnetwork, and thus there is a nonmonotonous varying of $R(\infty)$. We can understand the different growth patterns by studying high-degree nodes (hubs), which (i) are more likely to adopt the behavior than those in homogeneous network networks for small values of λ and (ii) lead to individuals adopting the
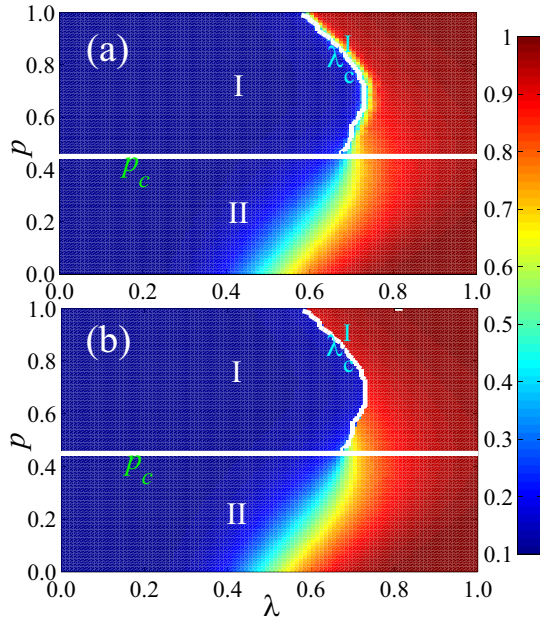
FIG. 6. Final behavior adoption size $R(\infty)$ versus information transmission probability λ and communication channels alternation probability p on uncorrelated ER-SF networks. Color-coded values of $R(\infty)$ from numerical simulations (a) and theoretical solutions (b) in the parameter plane (λ, p). The white horizontal line p_c separates the plane into regions I and II. In region I (II), $R(\infty)$ exhibits a hybrid (continuous) growth with λ. The white curves denote the theoretical discontinuous critical points λ_c^I. We set other parameters as $\langle k_\mathcal{A} \rangle = 10$, $\langle k_\mathcal{B} \rangle = 10$, $\upsilon_\mathcal{B} = 3.0$, $\rho_0 = 0.1$, and $T_\mathcal{A} = T_\mathcal{A} = 3$.
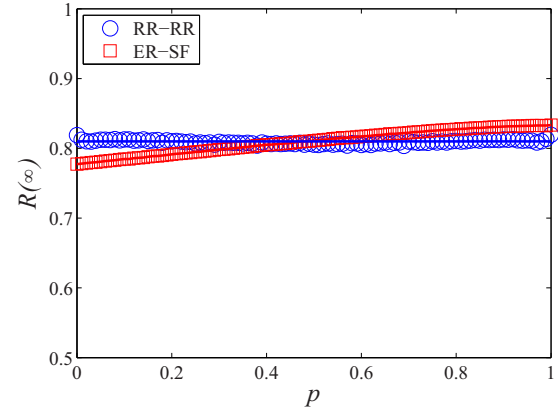

FIG. 7. Final behavior adoption size $R(\infty)$ versus communication channels alternation probability p on multiplex networks when $T_\mathcal{A} = T_\mathcal{B} = 1$. The symbols are the numerical simulation results, and lines are the theoretical predictions. We set other parameters as $\langle k_\mathcal{A} \rangle = 10$, $\rho_0 = 0.1$, $\langle k_\mathcal{B} \rangle = 10$, and $\upsilon_\mathcal{B} = 3.0$ for SF networks.

behavior gradually with fewer individuals in the subcritical state simultaneously adopting the behavior [34]. The fraction of hubs in the live subnetwork varies with p. We define a live subnetwork to be a user's active subnetwork at different time steps. For small $\lambda = 0.5$, individuals active in heterogeneous (homogeneous) networks can easily (with difficulty) adopt the behavior, adding the second role of hubs, and $R(\infty)$ thus decreases with p. For the larger $\lambda = 0.6$, $R(\infty)$ first decreases continuously because some individuals are active in heterogeneous networks when p is relatively small (e.g., $p < 0.5$), and $R(\infty)$ then increases discontinuously because many individuals are active in homogeneous networks and in the subcritical state for large p. The strange phenomena when $\lambda = 0.7$ is also induced by the live network. When $p \approx 0.4$, many individuals are active in homogeneous subnetwork $\mathcal{A}$, and $R(\infty)$ thus increases with p. A further increase of p is a slight perturbation that moves many individuals into the subcritical state, and $R(\infty)$ decreases discontinuously. When $\lambda = 0.8$, most individuals adopt the behavior, few individuals are in the subcritical state, and there is only a nonmonotonous varying of $R(\infty)$ versus p. These phenomena do not occur when $T_\mathcal{A} = T_\mathcal{B} = 1$, as shown in Fig. 7. We can predict these phenomena using our theoretical method. Note that the deviations near the discontinuous points can be eliminated by enlarging the network size N.

Figure 6 shows $R(\infty)$ versus the $\lambda - p$ plane. Using the growth pattern of $R(\infty)$ versus λ, we divide the plane into regions I and II according to a critical CCA probability

p_c. In region I, $R(\infty)$ first grows continuously with λ then increases discontinuously at λ_c, and in region II, $R(\infty)$ grows continuously with λ. There is thus a crossover phenomenon in the growth pattern: When $p > p_c$, the growth pattern of $R(\infty)$ is discontinuous; otherwise, it is continuous. We can explain the growth pattern of $R(\infty)$ using bifurcation theory. The discontinuous critical points λ_c^I exhibit a nonmonotonic change with p because of the CCA. When $p > p_c$, individuals are more likely to be active in subnetwork $\mathcal{A}$, and thus there are some hubs and many low-degree individuals in the live subnetwork. These hubs promote behavior adoption. Increasing p decreases the number of hubs and low-degree individuals in the live network, and p_c thus first increases and then decreases. The results from our theoretical method agree with those from the numerical simulations.

V. CONCLUSIONS

We have investigated how CCA affects the dynamics of social contagions. We first propose a non-Markovian behavior spreading model for multiplex networks in which each individual can only transmit and obtain the information from neighbors in their own subnetwork. To include CCA, we assume that an individual can be active in only one communication layer and at any given time can only transmit behavioral information to neighbors and read behavioral information from neighbors within the same subnetwork. The CCA slows a user's ability to receive information from both subnetworks. Thus time delays in obtaining the information from both subnetworks are introduced. We then perform numerical simulations of artificial multiplex networks and find that the time delays caused by CCA slow the behavior adoption process but do not affect the final behavior adoption size. In addition, CCA suppresses the final behavior adoption size $R(\infty)$ but does not change the growth pattern of $R(\infty)$ on RR-RR networks. We find in ER-SF networks that the growth pattern of $R(\infty)$ can be changed from hybrid to continuous by decreasing the layer-switching probability. To quantify the non-Markovian spreading dynamics, we develop

an edge-based compartmental method that produces results that agree with the numerical simulation results.

We have examined how CCA—an important interlayer switching mechanism—affects social contagions. We first construct the connections between human dynamics [57–59] and social contagions on multiplex networks. Individuals accomplishing different tasks using different communication channels do so in patterns that exhibits memory and burst characteristics. Our results here are the first to investigate the effects of human dynamics on social contagions in multiplex networks, and they expand our understanding of phase transition phenomena. The hybrid growth in the final adoption size is similar to the hybrid phase transition observed in other dynamics [60–62], and the critical phenomena of our proposed social contagions near the critical point need further investigation. Our theoretical method allows us to understand how CCA shapes spreading dynamics and to analyze different dynamic processes on multiplex networks. Our work may stimulate further research on social contagions that takes into account both realistic spreading mechanisms and network topologies and provides theoretical insights into how to control the spread of epidemics. In addition, social contagions with a heterogeneous layer-switching probability is an intriguing subject for examination [32]. For example, a layer-switching probability follows a power-law distribution, and the layer-switching probability of each individual is dependent on their inherent characteristics.

ACKNOWLEDGMENTS

APPENDIX A: NULL MODEL FOR SOCIAL CONTAGIONS WITH CCA

We use the layer-switching parameter p to describe CCA in the null model. The only difference between this null model and the model described in Sec. 2 is that in this null model we assume a susceptible individual becomes adopted when the accumulated units of received information is equal to or larger than the adoption threshold in any subnetwork, regardless of whether the individual is active in the subnetwork. This difference allows the susceptible individual to obtain the behavioral information without time delays. The null model includes CCA but not time delays.

APPENDIX B: $T_{\mathcal{A}} = T_{\mathcal{B}} = 1$

Figure 7 shows the contagions on multiplex networks with $T_{\mathcal{A}} = T_{\mathcal{B}} = 1$, i.e., the contagions on both subnetworks return to the simple contagion. We find that $R(\infty)$ does not change with p on RR-RR multiplex networks and increases with p on ER-SF networks.

[1] S. Boccaletti, G. Bianconi, R. Criado, C. I. Del Genio, J. Gómez-Gardeñes, M. Romance, I. Sendiña-Nadal, Z. Wang, and M. Zanin, Phys. Rep. **544**, 1 (2014).

[2] J. Gao, S. V. Buldyrev, H. E. Stanley, and S. Havlin, Nat. Phys. **8**, 40 (2012).

[3] G. D'agostino and A. Scala, *Networks of Networks: The Last Frontier of Complexity* (Springer, Berlin, 2014), Vol. 340.

[4] M. Kivelä, A. Arenas, M. Barthelemy, J. P. Gleeson, Y. Moreno, and M. A. Porter, J. Complex Netw. **2**, 203 (2014).

[5] J. Y. Kim and K.-I. Goh, Phys. Rev. Lett. **111**, 058702 (2013).

[6] F. Radicchi, Phys. Rev. X **4**, 021014 (2014).

[7] S. V. Buldyrev, R. Parshani, G. Paul, H. E. Stanley, and S. Havlin, Nature **464**, 1025 (2010).

[8] E. Cozzo, R. A. Banos, S. Meloni, and Y. Moreno, Phys. Rev. E **88**, 050801 (2013).

[9] A. Saumell-Mendiola, M. Á. Serrano, and M. Boguná, Phys. Rev. E **86**, 026106 (2012).

[10] X. Zhang, S. Boccaletti, S. Guan, and Z. Liu, Phys. Rev. Lett. **114**, 038701 (2015).

[11] E. H. W. Xu, W. Wang, C. Xu, M. Tang, Y. Do, and P. M. Hui, Phys. Rev. E **92**, 022812 (2015).

[12] G. J. Baxter, S. N. Dorogovtsev, A. V. Goltsev, and J. F. F. Mendes, Phys. Rev. Lett. **109**, 248701 (2012).

[13] M. Dickison, S. Havlin, and H. E. Stanley, Phys. Rev. E **85**, 066109 (2012).

[14] E. Cozzo and Y. Moreno, Phys. Rev. E **94**, 052318 (2016).

[15] M. A. Porter and J. P. Gleeson, in *Dynamical Systems on Networks* (Springer, Berlin, 2016), pp. 5–27.

[16] C. D. Brummitt, K.-M. Lee, and K.-I. Goh, Phys. Rev. E **85**, 045102 (2012).

[17] B. Min and K.-I. Goh, Phys. Rev. E **89**, 040802 (2014).

[18] O. Yağan and V. Gligor, Phys. Rev. E **86**, 036103 (2012).

[19] D. J. Watts, Proc. Natl. Acad. Sci. USA **99**, 5766 (2002).

[20] K.-M. Lee, C. D. Brummitt, and K.-I. Goh, Phys. Rev. E **90**, 062816 (2014).

[21] A. Majdandzic, L. A. Braunstein, C. Curme, I. Vodenska, S. Levy-Carciente, H. E. Stanley, and S. Havlin, Nat. Commun. **7**, 10850 (2016).

[22] A. Majdandzic, B. Podobnik, S. V. Buldyrev, D. Y. Kenett, S. Havlin, and H. E. Stanley, Nat. Phys. **10**, 34 (2014).

[23] W. Wang, Q.-H. Liu, S.-M. Cai, M. Tang, L. A. Braunstein, and H. E. Stanley, Sci. Rep. **6**, 29259 (2016).

[24] W. Wang, M. Tang, H. Yang, Y. Do, Y.-C. Lai, and G. Lee, Sci. Rep. **4**, 5097 (2014).

[25] Q.-H. Liu, W. Wang, M. Tang, and H.-F. Zhang, Sci. Rep. **6**, 25617 (2016).

[26] C. Granell, S. Gómez, and A. Arenas, Phys. Rev. Lett. **111**, 128701 (2013).

[27] S. Funk, E. Gilad, C. Watkins, and V. A. Jansen, Proc. Natl. Acad. Sci. USA **106**, 6872 (2009).

[28] P. Holme and J. Saramäki, Phys. Rep. **519**, 97 (2012).

[29] J. O. Haerter, B. Jamtveit, and J. Mathiesen, Phys. Rev. Lett. **109**, 168701 (2012).

[30] B. Min, S.-H. Gwak, N. Lee, and K.-I. Goh, Sci. Rep. **6**, 21392 (2016).

[31] M. De Domenico, A. Solé-Ribalta, S. Gómez, and A. Arenas, Proc. Natl. Acad. Sci. USA **111**, 8351 (2014).

[32] M. Starnini, A. Baronchelli, and R. Pastor-Satorras, Sci. Rep. **7**, 8597 (2017).

[33] M. Catanzaro, M. Boguñá, and R. Pastor-Satorras, Phys. Rev. E **71**, 027103 (2005).

[34] W. Wang, M. Tang, H.-F. Zhang, and Y.-C. Lai, Phys. Rev. E **92**, 012820 (2015).

[35] W. Wang, M. Tang, P. Shu, and Z. Wang, New J. Phys. **18**, 013029 (2016).

[36] W. Wang, P. Shu, Y.-X. Zhu, M. Tang, and Y.-C. Zhang, Chaos **25**, 103102 (2015).

[37] B. Schönfisch and A. de Roos, BioSystems **51**, 123 (1999).

[38] D. Centola, Science **334**, 1269 (2011).

[39] G. J. Baxter, S. N. Dorogovtsev, A. V. Goltsev, and J. F. F. Mendes, Phys. Rev. E **82**, 011103 (2010).

[40] G. J. Baxter, S. N. Dorogovtsev, A. V. Goltsev, and J. F. F. Mendes, Phys. Rev. E **83**, 051134 (2011).

[41] M. A. Di Muro, L. D. Valdez, S. V. Buldyrev, H. E. Stanley, and L. A. Braunstein, arXiv:1811.03995 (2018).

[42] W. Wang, M. Tang, H.-F. Zhang, H. Gao, Y. Do, and Z.-H. Liu, Phys. Rev. E **90**, 042803 (2014).

[43] J. C. Miller and E. M. Volz, PLoS ONE **8**, e69162 (2013).

[44] J. C. Miller, J. Math. Biol. **62**, 349 (2011).

[45] W. Wang, M. Tang, H. E. Stanley, and L. A. Braunstein, Rep. Prog. Phys. **80**, 036603 (2017).

[46] B. Karrer and M. E. J. Newman, Phys. Rev. E **82**, 016101 (2010).

[47] P. V. Mieghem, *Performance Analysis of Communications Systems and Networks* (Cambridge University Press, Cambridge, 2014).

[48] M. Newman, *Networks: An Introduction* (Oxford University Press, Oxford, 2010).

[49] S. H. Strogatz, *Nonlinear Dynamics and Chaos: With Applications to Physics, Biology, Chemistry, and Engineering* (Westview Press, Boulder, CO, 2014).

[50] J. P. Gleeson and D. J. Cahalane, Phys. Rev. E **75**, 056103 (2007).

[51] X. Yuan, Y. Hu, H. E. Stanley, and S. Havlin, Proc. Natl. Acad. Sci. USA **114**, 3311 (2017).

[52] R. Parshani, S. V. Buldyrev, and S. Havlin, Phys. Rev. Lett. **105**, 048701 (2010).

[53] P. Erdös and A. Rényi, Publ. Math. Inst. Hung. Acad. Sci **5**, 17 (1960).

[54] J. Gao, S. V. Buldyrev, S. Havlin, and H. E. Stanley, Phys. Rev. Lett. **107**, 195701 (2011).

[55] X. Liu, H. E. Stanley, and J. Gao, Proc. Natl. Acad. Sci. USA **113**, 1138 (2016).

[56] M. Boguná, R. Pastor-Satorras, and A. Vespignani, Eur. Phys. J. B **38**, 205 (2004).

[57] A.-L. Barabasi, Nature **435**, 207 (2005).

[58] A. Vazquez, Phys. Rev. Lett. **95**, 248701 (2005).

[59] D. Brockmann, L. Hufnagel, and T. Geisel, Nature **439**, 462 (2006).

[60] S. N. Dorogovtsev, A. V. Goltsev, and J. F. Mendes, Rev. Mod. Phys. **80**, 1275 (2008).

[61] M. A. Di Muro, L. Alvarez-Zuzek, S. Havlin, and L. Braunstein, New J. Phys. **20**, 083025 (2018).

[62] C. Wu, S. Ji, R. Zhang, L. Chen, J. Chen, X. Li, and Y. Hu, Europhys. Lett. **107**, 48001 (2014).